MINERALOGIA POLONICA
Vol. 31, No 2, 2000
PL ISSSN 0032-6267

Wojciech FRANUS[1], *Andrzej MANECKI*[1], *Tadeusz WIESER*[2]

RANCIEITE FROM CLINOPTILOLITE-MONTMORILLONITE CLAYSTONES OF THE SKOLE UNIT (THE POLISH FLYSCH CARPATHIANS)

Abstact. Four horizons with Mn-oxide concretions were encountered in Nowa Wieś near Rzeszów in the profile of the Variegated Shale Formation of the Flysch Carpathians. These horizons occur in the upper part of the profile, within the so-called clinoptilolite–montmorillonite clays. The predominating mineral of the concretion examined is rancieite (Mn-oxyhydroxide rich in Ca^{2+}) with the compositions established by scanning microprobe analysis: $(Na_{0.04}K_{0.07}Ca_{1.731}Mg_{0.133}Ba_{0.004}Al_{0.014}Fe^{2+}{}_{0.06})_{2.052}Mn^{4+}{}_{5.947}O_{13.93}\cdot(H_2O)_{5.67}$ for its individually occurring grains, and $(Na_{0.03}K_{0.075}Ca_{1.755}Mg_{0.148}Ba_{0.001}Al_{0.014}Fe^{2+}{}_{0.052})_{2.048}Mn^{4+}{}_{5.98}O_{13.94}\cdot(H_2O)_{5.72}$ for the grains intergrown with smectite. The Lower Eocene rancieites from Nowa Wieś exhibit the higher content of calcium ions (*ca* 85%) in interlayer positions and almost completely oxidized manganese known so far.

Key-words: rancieite, chemical composition, X-ray, IR, DTA, Polish Flysch Carpathians

INTRODUCTION

Rancieite, sometimes identified with birnessite, has in the last two decades been approved under its original mineral name. Chemically, it represents Ca-rich, hydrated, chiefly tetravalent manganese oxide, related in its sheet-like, hexagonal structure to birnessite, buserite and vernadite. X-ray diffraction patterns and IR spectra allow rather easily to differentiate the minerals mentioned.

Rancieites may appear under much varying environmental conditions. These are connected with: 1. hydrothermal action; 2. surface- and undersurface land weathering; 3. lacustrine and marine sediment diagenesis and redeposition, mainly under influence of initially reductional agents (organic matter) changing into oxidational ones (free oxygen). These two redox stages were rendered conspicuous by, eg., rhodochrosite micronodules changing to birnessite coatings to fully birnessitic micronodules (Wieser 1982, 1985).

[1] University of Mining and Metallurgy, al. Mickiewicza 30, 30-059 Kraków, Poland; e-mail: franus@poland.com

[2] Polish Geological Institute, Skrzatów 1, 31-560 Kraków, Poland.

Quantitatively, in comparison with other Mn minerals, rancieite forming Carpathian nodules is subordinate to rhodochrosite and birnessite but considerably prevails over todorokite (Gucwa, Wieser 1978). In the area belonging to the Skole tectonic unit of the Flysch Carpathians rancieite is almost a single Mn mineral in the clinoptilolite-montmorillonite-bearing, Lower Eocene Variegated Shale Formation. Rare microconcretions of the same age contain rhodochrosite (Wieser 1994), while in other formations of the Skole unit there occur nodules with Ca-Mg rhodochrosite (Muszyński et al. 1978).

GEOLOGICAL SETTING

The Red Shale Trójca Member (also called clinoptilolite-montmorillonite claystones) is situated in the upper part of the Variegated Shale Formation. The age of this formation ranges from Upper Palaeocene to Lower Eocene, and the Red Shale Trójca member occupies the middle part of Lower Eocene. The thickness of the Trójca Member reaches 20–30 m on the average, and that of the whole formation 130–190 m. Within the Skole Unit of the Carpathians the formation mentioned represents a series of clayey and clayey-silty red and green shales with lensoidal lithosomes of the Kosztowa sandstones in the middle part of the profile and other sandy members in its bottom (Boguszówka sandstones) and top (striped Chmielnik sandstones) parts. Lithosomes of the Babice clay (deposits of cohesive submarine flows) and the Bircza Lithotamnium Limestone Bed occur in the Palaeocene part of this formation (Rajchel 1990).

The Red Shale Trójca Member is composed almost exclusively of shales. They are distinguished from the under- and overlaying variegated strata by intensive cinnabar-like or brick-red colours. Hematite is responsible for the overall colour of these shales, although usually they also contain some intercalations of willow-green and green shales (layers from single to 15 or so millimetres), and small lithosomes of the Kosztowa sandstone. The presence of clinoptilolite, Radiolarian frustules and dispersed pyroclastic material are the most striking features of the Trójca Member (Wieser 1994).

In the prospecting trench in the vicinity of Nowa Wieś (SE of Rzeszów) four horizons with manganese concretions were found within the Trójca Member (Fig. 1). The concretions represent mostly the single-core type. Their sizes are strongly diversified: the largest reach a size of 6 × 7 × 5 cm, while the smallest are some millimetres across. They are usually bread-loaf-shaped, polygonal (5-, 6- or 7-sided), very often with strongly sculpted upper surfaces, but irregular forms were also spotted. The upper and lower crusts of the concretions are black-brown, from 2–5 mm to 3–4 cm thick, and the cores are ochre-orange coloured. The interiors of the nodules represent relicts of a sediment different than confining shales, certainly of fluxoturbiditic (horizons NW-18 and -22) or turbiditic (horizon NW-24) provenance. The more silty or even sandy (± glauconite) interiors show different stages of infiltration and replacement by rancieite and infrequent goethite (Phot. 1, 2).

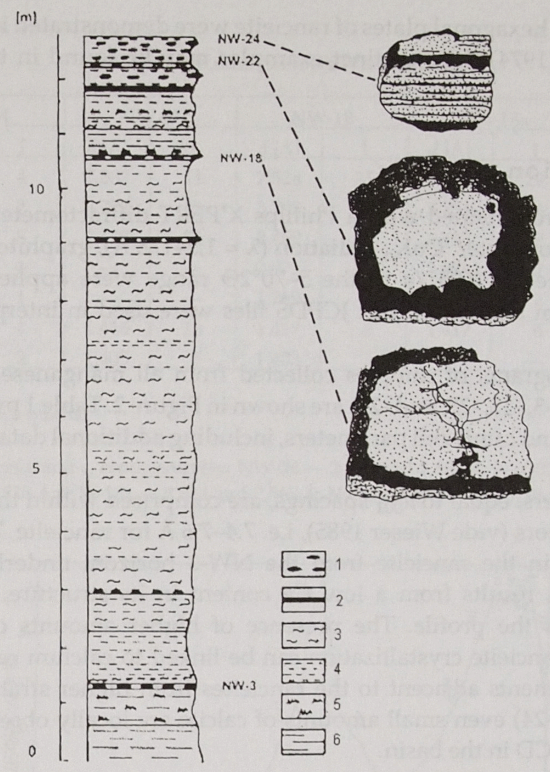

Fig. 1. Lithostratigraphic profile of Lower Eocene clinoptilolite-montmorillonite shaly claystones and confining sediments at Nowa Wieś, near Rzeszów. Also presented are rancieite nodule horizons, as well as exemplary nodule sections

1 — rancieite nodules, 2 — black shales, 3 — brick- to brown-red shaly claystones, 4 — green shales, 5 — ash-gray siltstones with Radiolaria, 6 — bluish ash-gray, Radiolaria-rich shales

EXPERIMENTAL AND RESULTS

Optical features

On the contrary to sometimes coexisting goethite of deeply brown colour, the rancieite is black with brownish tint. Only in very fine cleavage shreds is rancieite sufficiently thin to be translucent and to reveal optical properties. The index of refraction, up to now unknown, was determined as $N_{\omega} = 1.787 \pm 0.002$. This result is conformable with very low reflectivity (13%), intense pleochroism and red internal reflexes of rancieite (Renard, Boulége 1978). Accordingly with its structural features (hexagonal), rancieite is uniaxial, optically negative, with N_{ω} parallel to the dominant basal pinacoid faces and more or less distinct cleavage planes. Well developed, though subhedral hexagonal plates of rancieite were demonstrated in a SEM image by Finkelman et al. (1974). Less distinct examples may be found in the present paper (Phot. 3, 4).

X-ray diffraction analysis

X-ray data were obtained with a Phillips X'PERT diffractometer coupled on line with an IBM PC computer. CuK_α radiation (λ = 1,54178 Å), graphite monochromator, and counting speed = 0.05°/s in the 5–70°2Θ range were applied. The computer XRAYAN program and card-index JCPDS files were used in interpretation of X-ray patterns.

X-ray diffractograms of samples collected from all manganese nodule horizons investigated (NW-3, -18, -22, and -24) are shown in Figure 2. Table 1 presents *d* spacings, intensities, and *a* and *c* unit-cell parameters, including additional data for a nodule crust (NW-18a).

The *c* parameters, equal to d_{001} spacings, are comprised within the limits proposed by almost all authors (vide Wieser 1985), i.e. 7.4–7.6 Å for rancieite. The low value for the *c* parameter in the rancieite from the NW-3 horizon, underlain by silica-rich Radiolaria shales, results from a low Ca content in its structure, but these values increase upwards the profile. The presence of higher amounts of Ca ions in the environment of rancieite crystallization can be linked to calcium carbonate plankton casts. In the sediments adjacent to the rancieites from higher stratigraphic horizons (NW-22 and NW-24) even small amounts of calcite are locally observed, proving the lowering of the CCD in the basin.

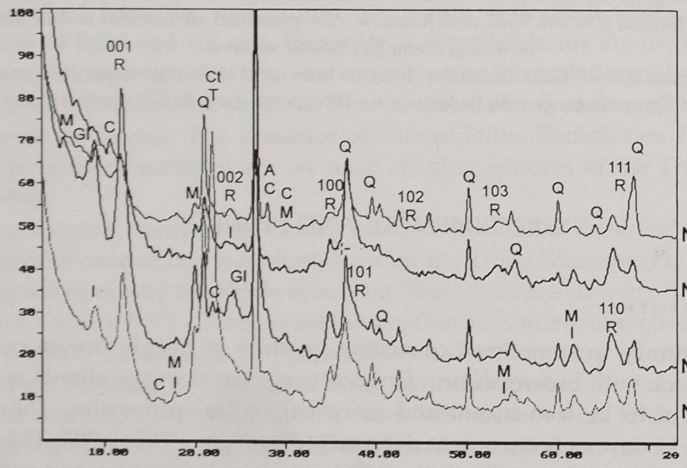

Fig. 2. X-ray patterns of manganese nodules from four horizons indicated in Figure 1
A — albite, C — clinoptilolite, Ct — low-cristobalite, Gl — glauconite, I — illite, M — montmorillonite, Q — quartz, R — rancieite, T — low-tridymite

TABLE 1

XRD powder data of Nowa Wieś rancieite

hkl	NW-24		NW-22		NW-18		NW-18a		NW-3	
	d [Å]	*I*	*d* [Å]	*I*	*d* [Å]	*I*	*d* [Å]	*I*	*d* [Å]	*I*
001	7.585	4	7.582	11	7.528	25	7.568	29	7.410	10
002	3.753	2	3.772	2	3.782	3	3.751	6	3.771	1
100*	2.456	8	2.452	54	2.459	15	2.453	29	2.461	7
102	2.068	1	—	—	2.072	2	2.074	2	—	—
103	1.740	1	—	—	1.760	2	1.761	2	—	—
110**	1.416	4	1.416	16	1.417	8	1.417	6	1.417	3
111**	1.408	2	1.405	5	1.403	3	—	—	1.405	3

* Coincidence with quartz.
** Diffuse reflexes.

Unit cell parameters a and c, representively: NW-24 — 2.832 and 7.585 Å; NW-22 — 2.832 and 7.582 Å; NW-18 — 2.834 and 7.528 Å; NW-18a — 2.834 and 7.568 Å; NW-3 — 2.834 and 7.410 Å.

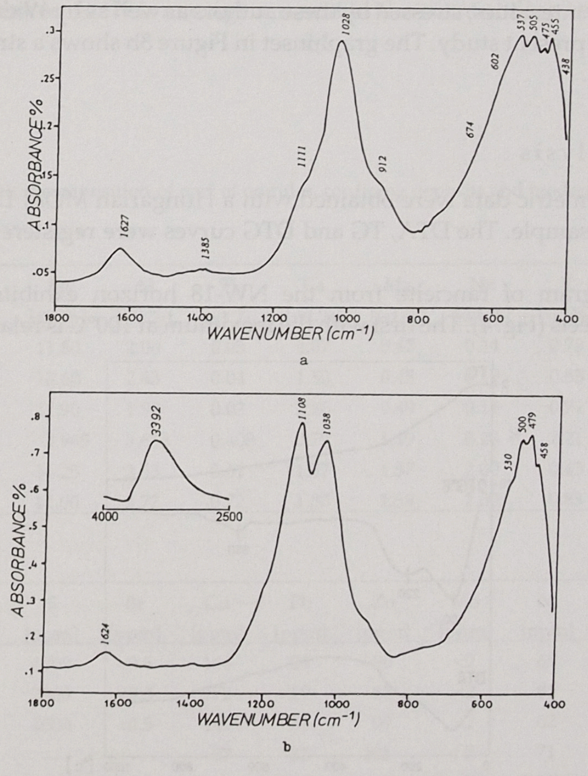

Fig. 3. Infrared absorption spectra of rancieites from the NW-18 (a) and NW-3 (b) horizons with quartz bands filtered out. The graph inset shows the broad water molecule stretching band

Broad reflexes 2.452–2.461 and 1.416–1.417 Å are characteristic of δ-MnO_2 (vernadite), now called and interpreted as disordered birnessite. This mineral is distinct by high optical dispersion and the highest oxidation of Mn^{3+} to Mn^{4+}. In EDS images (Phot. 3, 4) vernadite is visible in the matrix between idiomorphic rancieite crystals and as coatings on the nodule surface. Samples with higher amounts of rancieite contain more illite and an admixture of clinoptilolite.

Infrared spectroscopy

Infrared absorption spectra were recorded in the ranges 400–1800 and 2500–4000 cm^{-1} with an FTS BIO-RAD 165 spectrometer. Samples were prepared as pressed discs, using 1 mg of powdered material and 300 mg KBr.

Figure 3 exhibits two spectra of rancieite samples from NW-18 (a) and NW-3 (b) horizons in the better diagnostic 400–1800 cm^{-1} range. In the spectra, the Si-O bands of silicate minerals have been filtered out electronically to enhance those of the remaining minerals. The bands of rancieite occur at 455–458 and 500–505 cm^{-1} and do not depart much from the data reported by Potter and Rossman (1979) and Barrese et al. (1986). The ratio of their intensities, stressed by these authors as well as by Wieser (1985), is less indicative in the present study. The graphinset in Figure 3b shows a stretching band of water molecules.

Thermal analysis

Thermogravimetric data were obtained with a Hungarian MOM Derivatograph-C using a 500-mg sample. The DTA, TG and DTG curves were registered at the heating rate 10°/min.

The thermogram of rancieite from the NW-18 horizon exhibits three distinct endothermal effects (Fig. 4). The first with the maximum at 100°C is related to the loss of

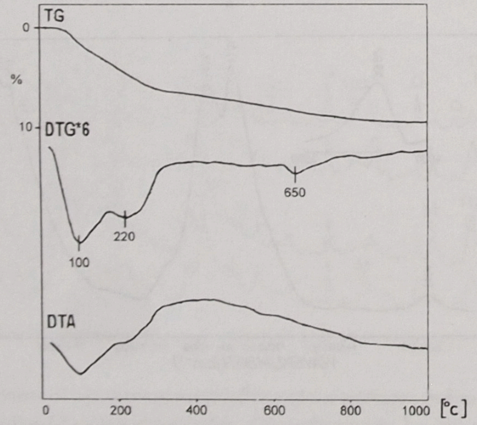

Fig. 4. Derivatogram of rancieite from the NW-18 horizon nodule crust

water adsorbed and loosely bound to the mineral structure (Barrese et al. 1986). This process is accompanied by a 7.6-% loss on weight. The other distinct endothermal effect, with the maximum at 220°C, is connected with the loss of constitutional water (5.8 wt.%). The total loss of these two effects is 13.4 wt.%, similar to that (13 wt.%) of the rancieite reported by Barrese et al. (1986). Much weaker loss on weight (1.8 wt.%) was recorded for the effect with the maximum at a temperature of 650ºC, interpreted as the destruction of the rancieite structure.

Chemical composition

Chemical compositions of the concretions studied and the enclosing sediment, as well as of some modern deep-sea concretions are presented in Table 2a–e. The manganese concretions from the Trójca red shales are distinctly depleted of heavy metals, e.g. Cu, Pb, Zn, Ni, Co, in comparison to their contemporaneous counterparts, while the Fe and Mn contents of the two are similar. There is no clear fractionation of metals in lower and upper parts of the concretion crusts. The REE composition of the Trójca concretions normalized to chondrite (Tab. 2e) reveals depletion of elements in relation to their average amount in the surrounding sediments in Nowa Wieś (Fig. 5).

TABLE 2

Chemical composition of part of nodules, confining deposits and modern nodules

a.

Sample	Mn [wt.%]	Fe [wt.%]	Al [wt.%]	Ti [wt.%]	Ca [wt.%]	Mg [wt.%]	Na [wt.%]	K [wt.%]	Ba [ppm]	Sr [ppm]
NW,1.	23.58	11.80	2.00	0.03	2.07	0.47	0.14	0.78	840	577
NW,m.	0.413	18.60	2.43	0.04	1.50	0.45	0.19	0.85	210	123
NW,u.	24.47	12.90	1.98	0.03	2.26	0.49	0.14	0.71	880	688
NW,d.	0.184	4.945	8.616	0.408	0.79	1.19	0.28	2.21	512	153
Ind.n.	16.36	14.25	2.63	0.61	1.57	1.57	2.00	0.43	1260	770
Pac.n.	21.08	11.00	2.72	0.72	1.80	1.58	2.00	0.83	2100	790

b.

Sample	P [ppm]	S [ppm]	Br [ppm]	Cu [ppm]	Pb [ppm]	Zn [ppm]	Mo [ppm]	Ni [ppm]	Sn [ppm]	Be [ppm]
NW,1.	2700	4000	<0.5	166	29	90	<2	69	<100	<2
NW,m.	2300	2000	<0.5	172	19	88	<2	81	<100	<2
NW,u.	1200	4000	<0.5	141	31	99	<2	62	<100	<2
NW,d.	6100	—	—	97	32	101	1.5	71	4.4	—
Ind.n.	—	—	—	0.17%	0.08%	0.07%	0.03%	0.39%	—	—
Pac.n.	0.25%	0.5%	—	0.59%	0.07%	0.10%	0.04%	0.80%	200	200

c.

Sample	Co [ppm]	Cd [ppm]	Rb [ppm]	Cs [ppm]	As [ppm]	Sb [ppm]	Bi [ppm]	Au [ppb]	Ag [ppm]	Hg [ppm]
NW,1.	79	<0.5	50	3	8.7	2.8	<5	8	<0.4	<1
NW,m.	53	0.5	47	2	4.9	0.8	<5	7	<0.4	<1
NW,u.	90	<0.5	<15	3	6.0	2.3	<5	11	<0.4	<1
NW,d.	28	—	129	7.9	9.0	1.0	0.83	—	–0.5	—
Ind.n.	0.2%	—	—	—	—	—	—	—	—	—
Pac.n.	0.27%	100	100	<100	1400	400	<100	<100	<100	<100

d.

Sample	Sc [ppm]	V [ppm]	Hf [ppm]	Cr [ppm]	Ta [ppm]	W [ppm]	Se [ppm]	Ir [ppb]	Th [ppm]	U [ppm]
NW,1.	7.5	8	2	35	<0.5	<1	3	<5	3.1	7.8
NW,m.	11.9	7	3	53	<0.5	<1	<3	<5	4.6	6.8
NW,u.	8.6	9	2	36	<0.5	2	<3	<5	3.5	9.0
NW,d.	—	102	3.4	98	0.92	3.4	—	—	13.6	1.6
Ind.n.	—	3700	—	—	—	—	–1	—	—	—
Pac.n.	<100	4500	100	400	—	1000	<100	<100	300	<100

e.

Sample	La [ppm]	Ce [ppm]	Nd [ppm]	Sm [ppm]	Eu [ppm]	Tb [ppm]	Er [ppm]	Yb [ppm]	Lu [ppm]	Y [ppm]
NW,1.	23.0	50	22	3.7	1.0	0.8	—	4.5	0.68	35
NW,m.	15.3	37	13	3.4	1.0	0.7	—	6.1	0.86	30
NW,u.	23.3	50	18	3.4	1.0	0.9	—	5.2	0.81	34
NW,d.	38.3	96.8	34.1	7.07	1.436	0.95	2.76	2.74	0.41	30
Ind.n.	163.4	885.96	69	31.56	6.85	7	—	12.43	2.19	62.3
Pac.n.	147.8	293.55	151.02	30.37	7.44	5.8	25.16	14.64	2.53	344.35

NW,1. — Nowa Wieś, lower part; NW,m. — Nowa Wieś, middle part; NW,u. — Nowa Wieś, upper part; NW,d. — Nowa Wieś, deposit; Ind.n. — Indian Ocean nodules; Pac.n. — Pacific Ocean nodules.

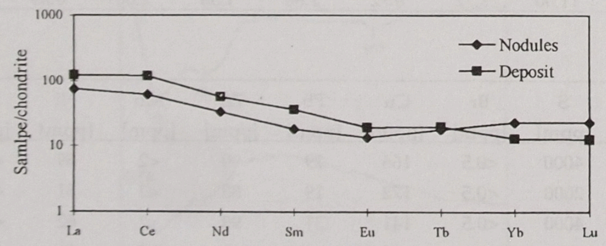

Fig. 5. Spiderdiagram of the incomplete REE sequence for mean composition of upper and lower parts of the nodule and confining sediment from the NW-18 horizon

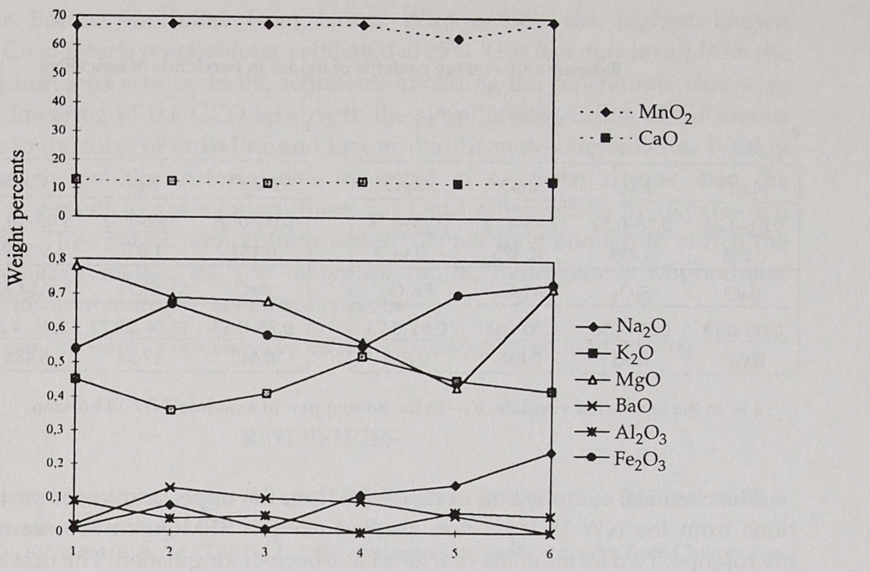

Fig. 6. Variability of some chemical elements in the rancieite grain (*cf.* Phot. 5) from the lowest bottom part of the NW-18 horizon nodule

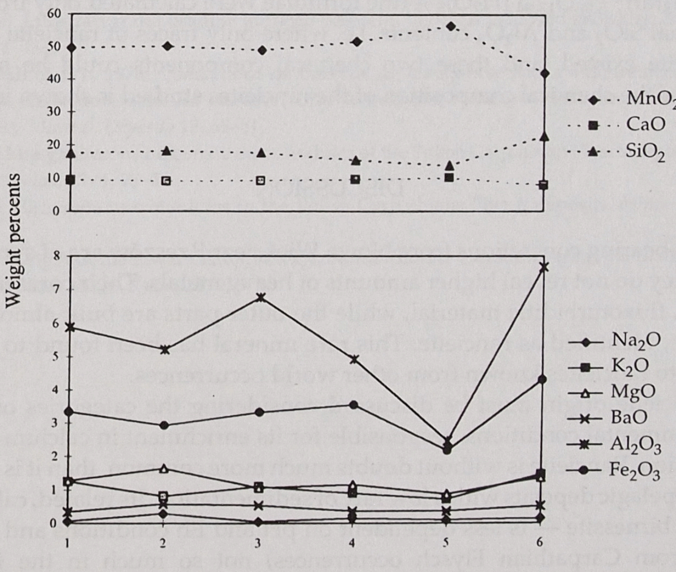

Fig. 7. Variability of some chemical elements in the rancieite grain (*cf.* Phot. 6) from the top part of the NW-18 horizon nodule

TABLE 3

Extreme and average contents of oxides in two kinds of rancieites

a.

Na_2O	K_2O	CaO	MgO
0.01–0.24	0.36–0.52	11.96–12.96	0.43–0.78
0.098	0.435	12.475	0.64
BaO	SiO_2	Al_2O_3	Fe_2O_3
0.00–0.13	0.37–0.56	0.00–0.09	0.54–0.73
0.065	0.43	0.048	0.628

b.

Na_2O	K_2O	CaO	MgO
0.06–0.28	0.72–1.47	8.06–10.16	0.87–1.64
0.132	1.037	9.278	1.227
BaO	SiO_2	Al_2O_3	Fe_2O_3
0.33–0.57	13.84–22.72	2.46–7.68	2.18–4.31
0.445	17.54	5.488	3.27

a — in the top part of a nodule, b — in the bottom part of a nodule. NW-18 horizon.

The chemical composition of rancietite from the upper and lower parts of a concretions from the NW-18 layer was studied using a SEMQuant 733 scanning electron microscope. Two forms of the rancieite have been distinguished. The first is represented by individual grains with the crystallochemical formula:

$(Na_{0.04}K_{0.07}Ca_{1.731}Mg_{0.133}Ba_{0.004}Al_{0.014}Fe^{2+}_{0.06})_{2.052}Mn^{4+}_{5.947}O_{13.93}\cdot(H_2O)_{5.67}$ (Fig. 6, Phot. 5). The other is developed as intergrowths of rancietite with smectite, and these areas reveal a distinct increase of SiO_2 and Al_2O_3 (Fig. 7, Phot. 6). The averaged crystallochemical formula of this form is $(Na_{0.03}K_{0.075}Ca_{1.755}Mg_{0.148}Ba_{0.001}Al_{0.014}Fe^{2+}_{0.052})_{2.048}Mn^{4+}_{5.98}O_{13.94}\cdot(H_2O)_{5.72}$ (the formulae were calculated only from the points with minimal SiO_2 and Al_2O_3 contents, i.e. where only traces of rancieite intergrowths with smectite existed, and these two chemical components could be omitted). The variability of the chemical composition of the rancieites studied is shown in Table 3.

DISCUSSION

The Mn-bearing concretions from Nowa Wieś near Rzeszów are of synsedimentary origin as they do not reveal higher amounts of heavy metals. Their cores are composed of a sandy, fluxoturbiditic material, while the outer parts are built almost entirely of a Mn-oxide, identified as rancieite. This rare mineral has been found to have similar properties to rancieites known from other world occurrences.

The rancieite origin must be discussed considering the categories of space, time and environmental conditions, responsible for its enrichment in calcium and efficient crystallization. Rancieite is without doubts much more common, than it is supposed, in oceanic, eupelagic deposits with a low rate of sedimentation. Its related, calcium-poorer mineral — birnessite — is less dependent on pH and Eh conditions and concentrates (judging from Carpathian Flysch occurrences) not so much in the form of macroconcretions but in micronodules, where calcium replaces alkalies with possible simultaneous oxidation of manganese.

The Lower Eocene rancieites from Nowa Wieś exhibit the highest known enrichment in Ca in interlayer positions, estimated at 85%. This fact may result from the increase of calcium ions activity in the sediments enclosing the concretions, due — in turn — to the lowering of the CCD level with the simultaneous influx of calcareous remnants, also in the form of turbiditic and fluxoturbiditic matrix ingredients. Weakly cemented Mn-rich, gel-like material was subjected in a greater degree than the turbidite-type sediment to granulation (Phot. 5, 6) and redeposition by oxygen-rich bottom currents. The contact with bottom water was not long enough to enrich the concretions in heavy metals, as it is in typical recent, hydrogenous Mn-nodules, called — not without a reason — metal scavengers.

Acknowledgements. The work was sponsored by the KBN (Warsaw), grant no. 6 P04D 022 16.

REFERENCES

BARRESE E., GIAMPAOLO C., GRUBESI O., MOTTANA A., 1986: Rancieite from Mazzano Romano (Latium, Italy). *Miner. Mag.* 50, 111–118.

FINKELMAN R.B., EVANS H.T.Jr., MATZKO J.J., 1974: Manganese minerals in geodes from Chihuachua, Mexico. *Miner. Mag.* 39, 549–558.

GUCWA I., WIESER T., 1978: Ferromanganese nodules in the Western Carpathian Flysch deposits of Poland. *Rocznik Pol. Tow. Geol.* 48, 147–182.

MUSZYŃSKI M., RAJCHEL J., SALAMON W., 1978: Concretionary iron and manganese carbonates in Eocene shales of the environs of Dynów near Przemyśl (Flysch Carpathians). *Miner. Polon.* 9, 111–122.

POTTER R.M., ROSSMAN G.R., 1979: Tetravalent manganese oxides: identification, hydration and structural relationships by infrared spectroscopy *Amer. Miner.* 64, 1199–1218.

RAJCHEL J., 1990: Litostratygrafia osadów górnego palecenu i eocenu jednostki skolskiej. *Z. Nauk. AGH*, Geologia 48, 1–114.

RENARD D., BOULÉGE J., 1978: Concretions de bioxyde de manganese sudes affleurements granitique dans une zone de balancement des marees. (Anse de Belmont, France) -1- analyse et mineralogie des encroutements. *Mineral. Deposita* 13, 65–81.

WIESER T., 1982: Manganiferous carbonate micronodules of the Polish Carpathian Flysch deposits and their origin. *Miner. Polon.* 13/1, 25–39.

WIESER T., 1985: Birnessite micronodules in the Polish Carpathians Flysch deposits. *Miner. Polon.* 16/2, 23–34.

WIESER T., 1994: Origin of the lower clinoptilolite-montmorillonite claystones from the Skole Unit of the Flysch Carpathians. *Miner. Polon.* 25/2, 3–20.

RANCIEIT Z IŁOWCÓW KLINOPTILOLITOWO-MONTMORILLONITOWYCH JEDNOSTKI SKOLSKIEJ (POLSKICH KARPAT FLISZOWYCH)

Streszczenie

W dolnoeoceńskich iłowcach klinoptilolitowo-montmorillonitowych w Nowej Wsi koło Rzeszowa stwierdzono występowanie czterech horyzontów z konkrecjami manganowymi. W składzie mineralnym tych konkrecji dominuje rancieit. Wyróżniono dwie jego odmiany o wzorach:

I — $(Na_{0.04}K_{0.07}Ca_{1.731}Mg_{0.133}Ba_{0.004}Al_{0.014}Fe^{2+}_{0.06})_{2.052}Mn^{4+}_{5.947}O_{13.93}\cdot(H_2O)_{5.67}$

II — $(Na_{0.03}K_{0.075}Ca_{1.755}Mg_{0.148}Ba_{0.001}Al_{0.014}Fe^{2+}_{0.052})_{2.048}Mn^{4+}_{5.98}O_{13.94}\cdot(H_2O)_{5.72}$.

Z drugą odmianą związane są zorientowane przerosty smektytu. Pochodzenie badanych konkrecji należy wiązać z procesami diagenezy, co podkreśla bardzo niska zawartość metali ciężkich w porównaniu do typowych głębokomorskich hydrogenicznych konkrecji z osadów współczesnych.

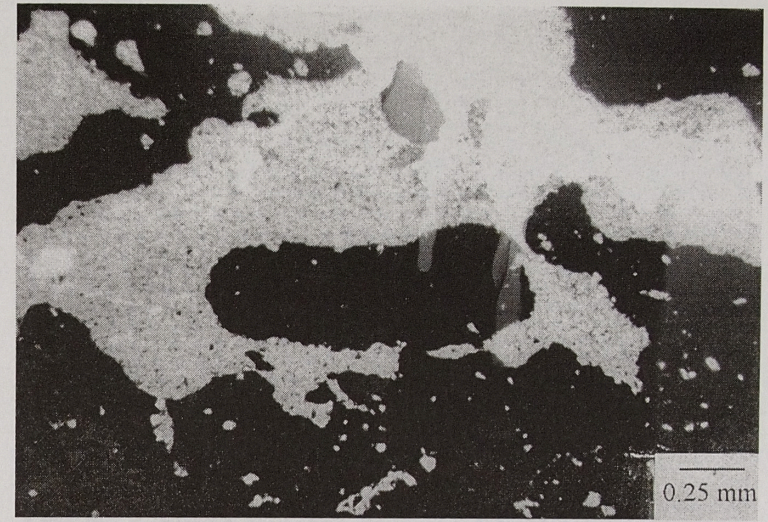

Phot. 1. Nodule section showing breccia-like structure with fragments composed, more or less exclusively, of rancieite. Upper part of the nodule is relatively rich in clayey and siliceous matrix. NW-3 horizon. One polarizer. Magn. 41×

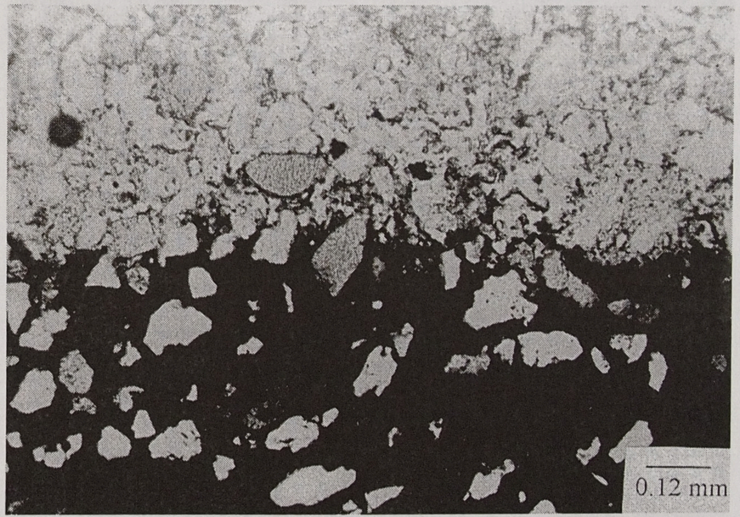

Phot. 2. Section perpendicular to the contact surface of internal, sandy fluxoturbiditic part and rancieitic external part of nodule. Near this surface two glauconite grains (gray) are located. NW-18 horizon. One polarizer. Magn. 89×

W. FRANUS, A. MANECKI, T. WIESER — Rancieite from clinoptilolite-montmorillonite claystones of the Skole unit (the Polish Flysch Carpathians)

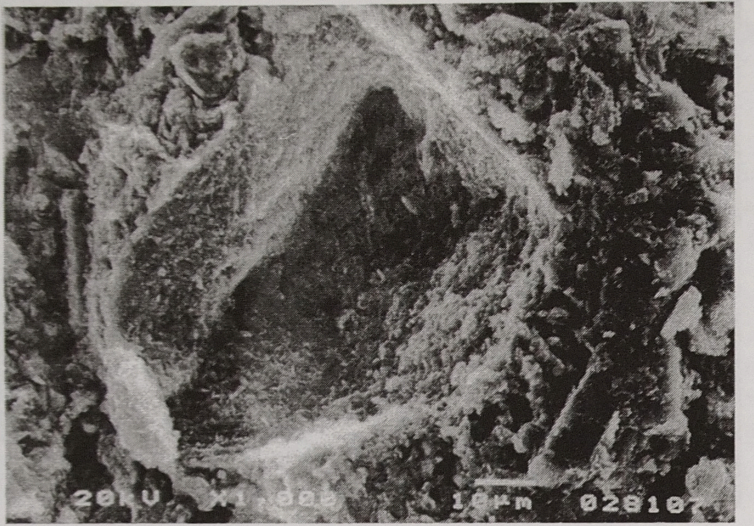

Phot. 3. Rancieite that appears as platy subhedral crystal with irregular hexagonal outlines. NW-18 horizon. SEM. Magn. 1000×

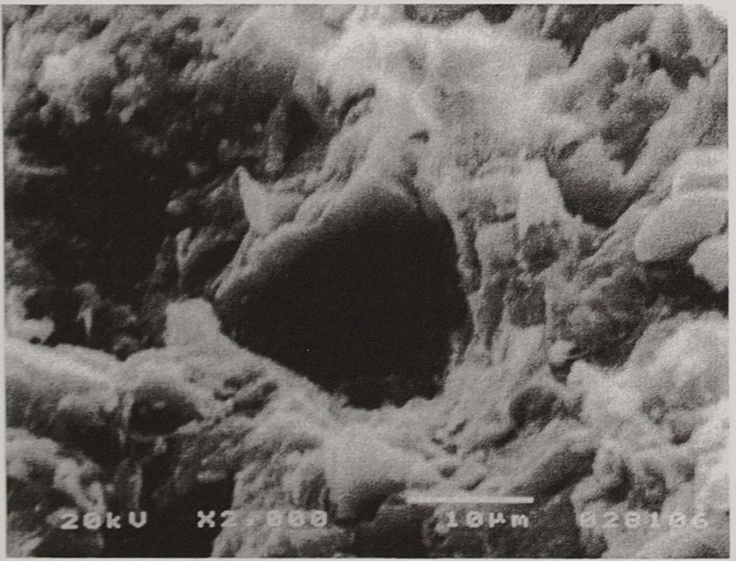

Phot. 4. Rancieite crystal (central position) embedded in rich clayey matrix. NW-18 horizon SEM. Magn. 2000×

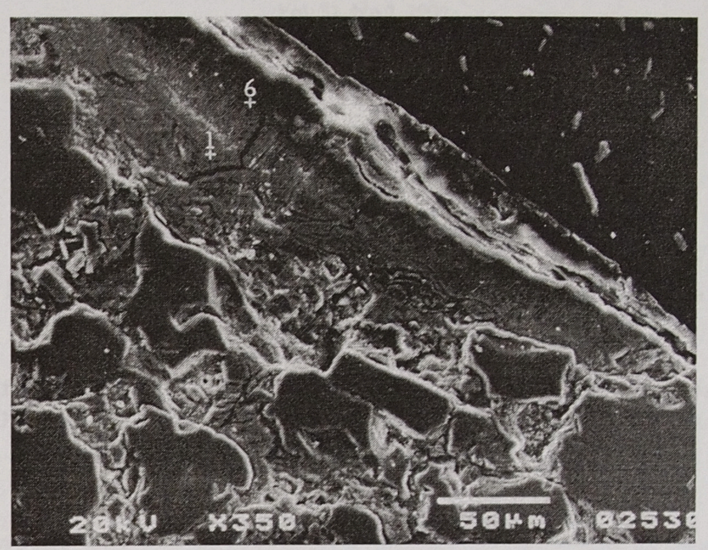

Phot. 5. Anhedral rancieite is in the upper left corner. Initial and final points of the scanning analytic profile (*cf.* Fig. 7) are indicated. NW-18 horizon, bottom part. SEM. Magn. 350×

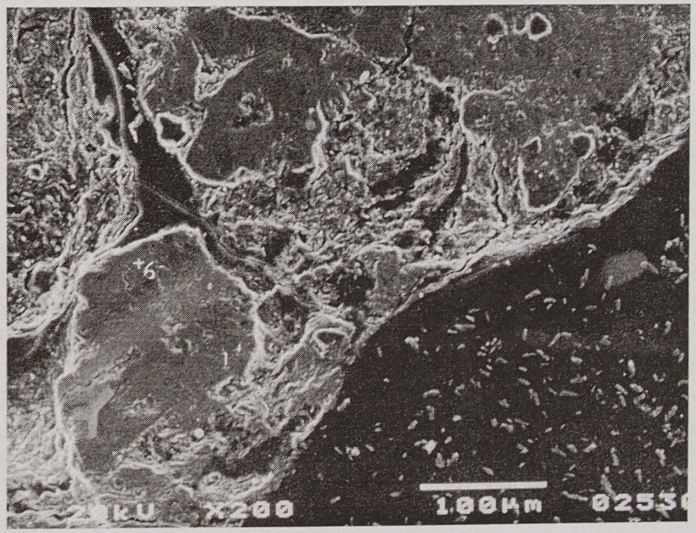

Phot. 6. Peculiar, anhedral and inhomogeneous grain of rancieite visible in the lower left corner (*cf.* Fig. 8). NW-18 horizon, top part. SEM. Magn. 200×